SIAM J. APPL. MATH.
Vol. 71, No. 2, pp. 540–558

WAVE ATTENUATION THROUGH MULTIPLE ROWS OF SCATTERERS WITH DIFFERING PERIODICITIES*

LUKE G. BENNETTS†

Abstract. A solution method is proposed for calculating wave scattering by a multiple-row array in which the rows are permitted to have different periodicities. Each individual row contains an infinite number of identical and equispaced scatterers, which can be solved through standard techniques by invoking periodicity. Previous studies have investigated the wave attenuation produced by multiple-row arrays but in which the periodicity in the rows is fixed. However, this leads to difficulties around the resonant points, at which the number of scattering angles produced by the rows changes. The method outlined in the present work involves a discretization of the directional spectrum. This is combined with a mapping of the individual rows onto neighboring geometries that fit into the discrete system so that, as the mesh is refined, the geometry converges to its intended form. The method is applied to a canonical problem in which a potential function exists in the two-dimensional plane exterior to an array composed of circular scatterers, which have a Neumann condition imposed on their boundaries. Forcing is provided by an incident wave. Wave attenuation is investigated in a numerical results section using ensemble averages in which the row spacings and in-row spacings are chosen from normal distributions. Convergence of the solutions with respect to the numerical method is established, and examples of the smoothing effects gained from incorporating variation in the in-row spacing are given.

Key words. wave scattering, diffraction, attenuation, periodicity, array

AMS subject classifications. 31A05, 31A10, 35Q35, 35Q60, 35Q86, 41A99

DOI. 10.1137/10080662X

1. Introduction.

Multiple-row arrays provide a computationally manageable means of calculating linear and time-harmonic wave fields traveling through a vast number of scatterers. They have been utilized in applications such as acoustic transmission in tube bundles [6], the calculation of electromagnetic properties of metallic and dielectric cylinders [12], water wave propagation through surface-piercing cylindrical obstructions [5], and the interaction of water waves with periodic topography [17]. Recently they have also been applied to determine the attenuation rates of ocean waves passing through the marginal ice zone produced from scattering by ice floes [3, 15, 1], and it is one of the findings of the most recent study in this sequence that provides the motivation for the current work.

The assumption that underpins the interaction theory in a multiple-row array is that each row is composed of an infinite number of evenly spaced and identical scatterers. Theoretical analysis of such a configuration (known in some applications as diffraction gratings) has provided stimulus for many of the leading figures in the area of wave scattering, beginning with [18]. Numerous works have since been published, and the prevailing approaches can be categorized into addition theorem methods [21], multipole methods [8], and quasi-periodic Green's function methods [16], each of which relies on invoking the periodicity of the problem. In addition to its extension

*Received by the editors August 26, 2010; accepted for publication (in revised form) January 6, 2011; published electronically March 31, 2011. This work was supported by the Marsden Fund Council from Government funding administered by the Royal Society of New Zealand, and by the Waves in Ice Forecasting for Arctic Operators project collaboratively funded by Total E&P and the Research Council of Norway.
http://www.siam.org/journals/siap/71-2/80662.html
†Department of Mathematics and Statistics, University of Otago, P.O. Box 56, Dunedin, 9054, New Zealand (lbennetts@maths.otago.ac.nz).

to multiple-row arrays, the single-row configuration has been successfully adapted to account for the effects of the boundary of the array, first for a semi-infinite row [9, 14] and later for a long, finite row [20].

There is a clear connection between a multiple-row array and a doubly periodic array [11]. Principally, the passing-band/stopping-gap structure that occurs in the latter is also evident in the former for a small number of approximately identical and equispaced rows [4, 11, 3, 15]. However, this does not resemble the exponential decay of waves that is observed through large collections of scatterers when randomness is significant, such as in the situation of ice floes in the marginal ice zone [19]. But, by creating an ensemble average in which the row spacings and the properties of the scatterers obey a Gaussian distribution, this behavior can be reproduced in most cases [15, 1].

In response to an incident plane wave, an individual row will transmit and reflect waves at a finite number of so-called scattering angles. The number and values of these scattering angles depend on the periodicity of the problem, which is determined by a relationship between the in-row spacing and the incident wave. Previous studies of multiple-row arrays have assumed that the periodicity (i.e., the in-row spacing) in each row is the same in order to restrict the wave interactions between rows to this set of angles. However, it was found in [1] that this assumption causes difficulties when attempting to calculate an attenuation rate around resonant points, at which the number of scattering angles changes. It is this phenomenon that is investigated in the current work.

A generalization in which the scatterers themselves are composed of a finite number of subscatterers is also possible [12, 15] and is a method that has elements in common with the technique that will be adopted here. But a common periodicity between the rows must still be maintained, and, to the author's knowledge, it has not been shown that this approach alleviates problems around the resonant points.

A canonical problem is considered here, in which a potential function exists in the two-dimensional plane exterior to an array of circular obstructions, on the perimeters of which a Neumann condition is imposed. An incident wave propagates towards the array and its diffracted form is sought. The rows that comprise the array are permitted to have different periodicities, which is accommodated in the solution procedure by discretizing the directional spectrum. An approximation is then formed by projecting the geometry in each row onto neighboring geometries, which have scattering properties that fit into the discrete framework. This enables the solutions for individual rows to be combined in an iterative manner to obtain the response of the entire array. As the discretization is refined, the geometry converges to its true state.

In the following section the mathematical setting for the above problem is defined. The solution method for a single row that is applied in this study is briefly reviewed at the beginning of section 3 and is followed by a description of the discrete framework for the interactions of multiple rows. Numerical results are presented in section 4. After a brief investigation for simple one- and two-row arrays, the results focus on ensemble averages of the transmitted wave field for a large number of rows, in which the row spacings and in-row spacings are selected from prescribed normal distributions. The results first verify that convergence is achieved as the resolution of the directional spectrum is increased, and then go on to illustrate the pronounced smoothing of the transmitted wave field that ensues from allowing variation in the periodicity of the rows. A modification of the solution method for a single row at the resonant points, which is based on the work of [10], is outlined in the appendix.

2. Preliminaries. We consider wave scattering in an infinite two-dimensional plane defined by the Cartesian coordinates $\mathbf{x} = (x, y)$. Occupying this domain is an array composed of a finite number of rows, M, say, each containing an infinite number of circular scatterers (or obstructions). In the exterior to these obstructions, Ω, say, it is assumed that a potential function exists, for which we seek a time-harmonic solution $\Re\mathrm{e}\{\phi(\mathbf{x})\mathrm{e}^{-\mathrm{i}\omega t}\}$ at a given frequency ω. The complex function ϕ satisfies the Helmholtz equation throughout the exterior domain, that is,

$$(\nabla^2 + k^2)\phi = 0 \quad (\mathbf{x} \in \Omega),$$

where k is a wavenumber, related in some manner to ω, and we assume that $k \in \mathbb{R}^+$. As the intention of this work is to study the interactions between rows, on the boundaries, Γ, say, of the obstructions, we choose to impose the simple Neumann condition

$$\partial_n \phi = 0 \quad (\mathbf{x} \in \Gamma).$$

The governing equations therefore represent wave scattering by rigid obstructions: either acoustic, or electromagnetic, or of reduced potential water waves. The corresponding Dirichlet problem could just as easily have been prescribed, and it has relevance in the former two application areas. Moreover, the method that will be outlined can be adapted to the situation of water wave scattering by an array of floating elastic plates, which provided the motivation for this work.

The obstructions in a particular row are identical and evenly spaced. Without loss of generality, we suppose that the rows are aligned with the y-axis, so that they may be counted in ascending order with respect to the x-axis. Let row m contain obstructions of radius r_m and suppose that one of these is centered at the point $\mathbf{x}_m = (x_m, 0)$. As the rows may not overlap, the row spacing $q_m = x_{m+1} - x_m$ must satisfy $q_m \geq r_m + r_{m+1}$ $(m = 1, \dots, M-1)$. If the spacing between centers of adjacent obstructions in a row, hereinafter known as the in-row spacing, is denoted $s_m \geq 2r_m$, then the centers of the obstructions in row m are situated at the points $\mathbf{x}_m + j(0, s_m)$ $(j \in \mathbb{Z})$. It is possible to consider a realignment in which the second component of each $\mathbf{x}_m$ is nonzero [3], but, as it is not expected to have a significant influence on our study, this freedom is abandoned in favor of presentational ease. An example of the geometry just described is shown in Figure 2.1.

Forcing is provided by an incident wave, ϕ_i, which propagates from $x \to -\infty$ towards the array. For what is to follow, it will be advantageous to consider forcing across the directional spectrum from the outset, that is, a sum of waves traveling at all possible angles. The incident wave is therefore of the form

$$\phi_i(\mathbf{x}) = \int_{-1}^{1} \iota(u)\mathrm{e}^{\mathrm{i}k(vx+uy)}\,\mathrm{d}u, \tag{2.1}$$

in which u is a nondimensional angle parameter, $v = v(u) = \sqrt{1-u^2} \in \mathbb{R}^+$, and ι is some prescribed amplitude function.

For a plane incident wave at the oblique angle τ (with respect to the x-axis, see Figure 2.1), which is denoted

$$\phi_i(\mathbf{x} : u_0) = \mathrm{e}^{\mathrm{i}k(v_0 x + u_0 y)},$$

where $u_0 = u_0(\tau) = \sin\tau$ and $v_0 = v_0(\tau) = \cos\tau = \sqrt{1-u_0^2}$, the amplitude function is given by $\iota = \delta(u - \sin\tau)$, where δ is the Delta function. During the scattering

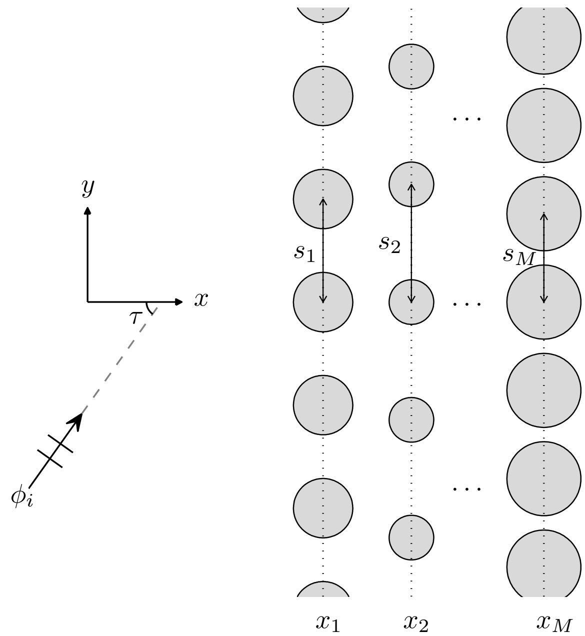

FIG. 2.1. *Schematic of the geometry.*

process the energy carried by the incident wave is redistributed across the directional spectrum, with a proportion being reflected and a proportion being transmitted. Exponentially decaying evanescent motions are also generated and are defined by $|u| > 1$ and $v \in \mathrm{i}\mathbb{R}^+$. The potential is therefore represented on either side of the array as

$$\phi(\mathbf{x}) = \phi_i(\mathbf{x}) + \int_{-\infty}^{\infty} a(u)\mathrm{e}^{-\mathrm{i}k(vx-uy)}\,\mathrm{d}u \quad (x < x_0 - r_1) \tag{2.2a}$$

and

$$\phi(\mathbf{x}) = \int_{-\infty}^{\infty} b(u)\mathrm{e}^{\mathrm{i}k(vx+uy)}\,\mathrm{d}u \quad (x > x_M + r_M), \tag{2.2b}$$

in which a and b are reflection and transmission amplitude functions, respectively, that are to be calculated. In the far-field the evanescent waves have decayed, and the potential reduces to the propagating wave components, so that

$$\phi(\mathbf{x}) \sim \phi_i(\mathbf{x}) + \int_{-1}^{1} a(u)\mathrm{e}^{-\mathrm{i}k(vx-uy)}\,\mathrm{d}u \quad (x \to -\infty)$$

and

$$\phi(\mathbf{x}) \sim \int_{-1}^{1} b(u)\mathrm{e}^{\mathrm{i}k(vx+uy)}\,\mathrm{d}u \quad (x \to \infty).$$

3. Formulation.

3.1. A single row. A number of efficient methods have been devised for the single-row problem (see [21, 8, 16, 2], for example), all of which rely on invoking the periodicity of the problem. Specifically, for a row with spacing s and a plane incident wave of angle τ, a quasi-periodic potential is sought, such that

$$\phi(x, y + s : u_0) = \mathrm{e}^{\mathrm{i}sku_0}\phi(x, y : u_0), \tag{3.1}$$

so that the solution need only be calculated in one strip of length s in the y-direction in order to obtain the solution throughout the entire domain. (Notice that we emphasize the dependence of the solution on the angle of the incident wave through the parameter u_0.) For solution purposes, we choose this strip to be $\Omega_0 = \{\mathbf{x} : x \in \mathbb{R}, |y| < s/2, |\mathbf{x}| \geq r\}$, which contains a single (whole) obstruction, and we assume that this obstruction is centered on the origin and has radius r.

In this work a modified version of the solution method outlined in [2] will be utilized. This involves an application of a quasi-periodic Green's function $G = G(\mathbf{x}|\mathbf{X} : u_0)$ (see [13, 7]) using the source point $\mathbf{X} = (X, Y)$, which corresponds to the field point $\mathbf{x}$. This function may be expressed as

$$G(\mathbf{x}|\mathbf{X} : u_0) = \frac{1}{2\mathrm{i}ks}\sum_{j=-\infty}^{\infty}\frac{1}{v_j}\mathrm{e}^{\mathrm{i}kv_j|x-X|-\mathrm{i}ku_j(y-Y)}, \tag{3.2}$$

where, if we define the nondimensional periodicity parameter $p = 2\pi/ks$, the quantities

$$u_j = u_j(u_0) = u_0 + jp, \quad v_j = v_j(u_0) = \sqrt{1 - u_j^2} \quad (j \in \mathbb{Z})$$

are constant for a given incident angle and extend the definitions of u_0 and v_0 given in the previous section. Using Green's second identity, the potential can be expressed as a sum of the incident wave and a convolution of the Green's function and itself, where the integral is taken around the boundary of the obstruction $\Gamma_0 = \{|\mathbf{x}| = r, -\pi < \theta \leq \pi\}$, with θ being the regular azimuthal coordinate. Specifically,

$$\epsilon\phi(\mathbf{X} : u_0) = \phi_i(\mathbf{X} : u_0) - r\int_{-\pi}^{\pi}[\partial_n G(\mathbf{x}|\mathbf{X} : u_0)\phi(\mathbf{x} : u_0)]_{|\mathbf{x}|=r}\,\mathrm{d}\theta \quad (\mathbf{X} \in \Omega_0), \tag{3.3}$$

where $\epsilon = 1$ if $\mathbf{x} \notin \Gamma_0$ and $\epsilon = 0.5$ if $\mathbf{x} \in \Gamma_0$. The potential is obtained by allowing the field point $\mathbf{x}$ tend to Γ_0 in (3.3) and solving the resulting integral equation via a Fourier expansion of the azimuthal coordinate.

Of particular note in the single-row problem, with plane wave forcing, is that the scattered field can be expressed as a discrete sum, consisting of a finite number of propagating waves and an infinite number of evanescent waves. For the incident plus reflected field this sum takes the form

$$\phi(\mathbf{x} : u_0) = \phi_i(\mathbf{x} : u_0) + \sum_{j=-\infty}^{\infty}\hat{R}_j\mathrm{e}^{\mathrm{i}k(-v_jx+u_jy)} \quad (x < -r),$$

and the transmitted field is similarly

$$\phi(\mathbf{x} : u_0) = \sum_{j=-\infty}^{\infty}\hat{T}_j\mathrm{e}^{\mathrm{i}k(v_jx+u_jy)} \quad (x > r),$$

where $\hat{R}_j = \hat{R}_j(u_0)$ and $\hat{T}_j = \hat{T}_j(u_0)$ are reflection and transmission coefficients, respectively, that can be calculated once ϕ is obtained on the boundary. The real values of the set $\{v_j : j \in \mathbb{Z}\}$ define the propagating scattered waves and determine their directions, known as the scattering angles. All other values of v_j are purely imaginary and define evanescent waves. It is clear that the incident angle is always in the set of scattering angles (through v_0). Multiple scattering angles will exist, for some range of incident angles τ, only if the nondimensional parameter $p \leq 2$, which is governed by a relationship between the in-row spacing s and the wavenumber k. When $p \leq 2$ the number of scattering angles will change as τ is varied.

At the points at which the number of scattering angles changes, either one or two values of $v_j = 0$, which defines waves that travel parallel to the row. As these points are approached the reflection and transmission amplitudes possess resonant behavior (see [8, 2]). They are therefore influential to the interaction theory that will be outlined in the following section, but it is clear from the representation of the Green's function (3.2) that the solution method is unsuitable in its present form for these situations. However, a solution can be obtained through some straightforward modifications. The details of these modifications are contained in the appendix and owe much to the work of [10].

The solution for a more general forcing, as in (2.1), can be obtained by superposing the plane wave solutions in the form

$$\phi(\mathbf{x}) = \int_{-1}^{1} \iota(u)\phi(\mathbf{x} : u)\ \mathrm{d}u.$$

The corresponding reflection and transmission amplitude functions are similarly deduced from

$$a(u) = \sum_{j=-\infty}^{\infty} \iota(u - pj)\hat{R}_j(u - pj), \quad b(u) = \sum_{j=-\infty}^{\infty} \iota(u - pj)\hat{T}_j(u - pj),$$

where the definition of the incident amplitude function has been extended to $\iota(u) = 0$ for $|u| > 1$. It will be more convenient to express the relationship between the reflected or transmitted amplitude function and the incident amplitude function in the form

$$a(u) = \int_{-\infty}^{\infty} R(u : u_0)\iota(u_0)\ \mathrm{d}u_0, \quad b(u) = \int_{-\infty}^{\infty} T(u : u_0)\iota(u_0)\ \mathrm{d}u_0,$$

where the reflection and transmission functions, R and T, respectively, give the response at u to the forcing at u_0 and are defined by

$$R(u : u_0) = \sum_{j=-\infty}^{\infty} \delta(u - u_j)\hat{R}_j(u_0), \quad T(u : u_0) = \sum_{j=-\infty}^{\infty} \delta(u - u_j)\hat{T}_j(u_0).$$

It should be noted that a solution that satisfies condition (3.1) is not necessarily unique, as Rayleigh–Bloch waves may exist for certain frequencies. Rayleigh–Bloch waves travel along the row with some other periodicity and decay exponentially with distance away from it. They would therefore be disregarded in the interaction theory implemented between the rows in this study. Furthermore, they typically exist only for $k < \pi/s$ [16], which is the regime in which only a single scattering angle is generated.

3.2. Multiple rows. If each row has the same in-row spacing $s_m = s$ ($m = 1, \ldots, M$), then, for a plane incident wave, the scattering angles supported between each pair of adjacent rows, and hence those generated by the full array, will be the same as the scattering angles produced by an individual row. Based on this, efficient interaction methods have been developed [5, 6, 12, 17, 15, 3]. However, it has been shown recently [1], in the context of wave scattering in a large field of ice floes, that the in-row spacing restriction produces unwanted effects around the resonant angles ($v_j = 0$) when calculating attenuation through the array, and it is this finding that motivates the present investigation.

In the current model the in-row spacings s_m $(m = 1, \ldots, M)$ in the array are permitted to differ, and the corresponding nondimensional periodicity parameters are denoted $p_m = 2\pi/ks_m$ $(m = 1, \ldots, M)$. When two rows with different in-row spacings are combined, the set of scattering angles generated through their interactions is governed by the periodicity parameter produced by the in-row spacing that is equal to the lowest common multiple of the two component in-row spacings. If no such multiple exists, then waves will travel across the directional spectrum. To keep track of the scattering angles for more than two rows, this process must be repeated in a systematic way for each additional row, and the numerical expense incurred in performing this task for every new array would be significant. Moreover, for arrays composed of many rows with randomized properties, which are of interest when calculating attenuation, the set of scattering angles can be expected to either become large enough to make dealing with each individual angle computationally inefficient, or become infinite, in which case there is no established interaction theory between rows. To avoid these severe drawbacks, an approximation method will be proposed, which fixes the scattering angles according to a specified tolerance, irrespective of the arrays under consideration.

Prior to introducing this approximation, it is pertinent to consider the structure of the wave field between adjacent rows. As an incident wave field of the form given in (2.1) has been set, it is appropriate to allow for waves traveling back and forth across the directional spectrum and also exponentially decaying at all possible rates. The potential between rows m and $m+1$ is therefore expressed as

$$\phi(\mathbf{x}) = \int_{-\infty}^{\infty} \left\{ a_m(u)\mathrm{e}^{-\mathrm{i}k(vx-uy)} + b_m(u)\mathrm{e}^{\mathrm{i}k(vx+uy)} \right\} \,\mathrm{d}u,$$

where a_m and b_m $(m = 1, \ldots, M-1)$ are the leftward and rightward traveling amplitude functions, respectively, and include waves decaying in that direction. At the ends of the array, the representations (2.2a)–(2.2b) hold, and, for consistency, the notations $a_0 = a$ and $b_M = b$ are used for the unknown scattered amplitude functions, and $b_0 = \iota$ and $a_M = 0$ are used for the known incident amplitude functions.

Let the reflection and transmission functions for row m be denoted R_m and T_m, respectively. The amplitude function b_m is associated with an incident wave for row $m+1$ and a scattered wave for row m, and, vice versa, a_m is associated with an incident wave for row m and a scattered wave for row $m+1$. It follows, noting the symmetry of the individual rows, that we may express the amplitude functions as

(3.4a)
$$a_{m-1}(u) = \int_{-\infty}^{\infty} \left\{ \mathrm{e}^{-\mathrm{i}(v_0+v)x_m} R_m(u:u_0) b_{m-1}(u_0) + \mathrm{e}^{\mathrm{i}(v_0-v)x_m} T_m(u:u_0) a_m(u_0) \right\} \mathrm{d}u_0$$

and

(3.4b)
$$b_m(u) = \int_{-\infty}^{\infty} \left\{ \mathrm{e}^{-\mathrm{i}(v_0-v)x_m} T_m(u:u_0) b_{m-1}(u_0) + \mathrm{e}^{\mathrm{i}(v_0+v)x_m} R_m(u:u_0) a_m(u_0) \right\} \mathrm{d}u_0$$

for $m = 1, \ldots, M$, where $v = v(u)$ and $v_0 = v(u_0)$. The exponential functions that appear in these expressions account for the phase changes incurred by having the row located at x_m rather than on the y-axis. The above identities (3.4a)–(3.4b) ($m = 1, \ldots, M$) give a set of $2M$ equations, which will be used to obtain the $2M$ unknown amplitude functions a_{m-1} and b_m ($m = 1, \ldots, M$).

Before proceeding, let a wide (row) spacing approximation (WSA) be invoked, which supposes that

$$\phi(\mathbf{x}) \approx \int_{-1}^{1} \left\{ a_m(u)\mathrm{e}^{-\mathrm{i}k(xv-yu)} + b_m(u)\mathrm{e}^{\mathrm{i}k(xv+yu)} \right\} \mathrm{d}u \tag{3.5}$$

at the point at which wave interactions take place between rows m and $m+1$. It is therefore assumed that all significant wave interactions involve only propagating waves. This can easily be adapted to include a proportion of the evanescent waves by extending the interval of integration in the approximation (3.5). However, the WSA has been shown to give high accuracy in related problems [15, 3], and for the purposes of this study it is considered sufficient.

The method that is used to obtain the amplitude functions from (3.4a)–(3.4b) is based on a discretization of the directional spectrum. This entails dividing the interval $u \in [-1, 1]$ into the set of evenly distributed points $\{u_{(n)} = n/N : n = -N, \ldots, N\}$, which is represented by the vector

$$\mathbf{u} = [u_{(-N)}, \ldots, u_{(N)}]^T.$$

The discretization parameter N is an arbitrary finite integer and is chosen large enough to achieve the desired accuracy.

For the scattering angles produced by the rows to fit into this discrete system, a discretization of the periodicity parameter spectrum is also required. Projecting the periodicity parameters, p_m, onto this mesh defines a set of approximate periodicity parameters to be

$$\tilde{p}_m = \frac{\lfloor p_m N \rceil}{N} \quad (m = 1, \ldots, M),$$

where $\lfloor \cdot \rceil$ denotes the nearest integer. These approximate values are produced by mapping the geometry in each row onto the neighboring geometry with radii $\tilde{r}_m = p_m r_m/\tilde{p}_m$ and in-row spacings $\tilde{s}_m = p_m s_m/\tilde{p}_m$. This is, in effect, imposing an artificial periodicity on the array, with a corresponding periodicity parameter $\tilde{p} = 1/N$. As the discretization parameter N is increased the approximate geometries and periodicities return to their original values. The problems posed by the approximate geometries are solved for each of the individual rows for all points in $\mathbf{u}$, noting that it is necessary only to solve on the interval $u_{(n)} \in [0, \tilde{p}/2]$ if $\tilde{p} < 2$ and $u_{(n)} \in [0, 1]$ if $\tilde{p} \geq 2$ to obtain the required reflection and transmission coefficients due to symmetry and periodicity.

For the interactions of the rows, the discrete analogues of (3.4a)–(3.4b) are

$$\mathbf{a}_{m-1} = \mathcal{E}_{m-}\mathcal{R}_m\mathcal{E}_{m-}\mathbf{b}_{m-1} + \mathcal{E}_{m-}\mathcal{T}_m\mathcal{E}_{m+}\mathbf{a}_m$$

and

$$\mathbf{b}_m = \mathcal{E}_{m+}\mathcal{T}_m\mathcal{E}_{m-}\mathbf{b}_{m-1} + \mathcal{E}_{m+}\mathcal{R}_m\mathcal{E}_{m+}\mathbf{a}_m,$$

respectively, for $m = 1, \ldots, M$. The length $2N+1$ vectors $\mathbf{a}_m$ and $\mathbf{b}_m$ contain the approximate values of the amplitude functions on the mesh $\mathbf{u}$, that is,

$$\mathbf{a}_m \approx a_m(\mathbf{u}), \quad \mathbf{b}_m \approx b_m(\mathbf{u})$$

for $m = 0, \ldots, M$. The dimension $2N+1$ square matrices $\mathcal{R}_m$ and $\mathcal{T}_m$ are the discrete versions of the reflection and transmission functions R_m and T_m, respectively, and are calculated using the approximate geometries. They are defined by

$$\{\mathcal{R}_m\}_{j,i} = R_m(u_{(j-N-1)} : u_{(i-N-1)}), \quad \{\mathcal{T}_m\}_{j,i} = T_m(u_{(j-N-1)} : u_{(i-N-1)})$$

for $i, j = 1, \ldots, 2N+1$ and $m = 1, \ldots, M$. The phase changes are contained in the diagonal matrices $\mathcal{E}_{m\pm} = \mathrm{diag}\{\mathrm{e}^{\pm \mathrm{i}\mathbf{v}x_m}\}$, where the vector $\mathbf{v} = \sqrt{1-\mathbf{u}^2}$ is the discrete version of the function v.

The solution method now proceeds in a fashion similar to that often used in the fixed in-row spacing problem, that is, by combining the equations for each row in an iterative manner. Therefore, let the discrete reflection and transmission matrices that operate over rows i to j ($i \leq j$) be denoted by $\mathcal{R}_{i,j}^{(\pm)}$ and $\mathcal{T}_{i,j}^{(\pm)}$, respectively. They are defined by

$$\mathbf{a}_{i-1} = \mathcal{R}_{i,j}^{(-)}\mathbf{b}_{i-1} + \mathcal{T}_{i,j}^{(+)}\mathbf{a}_j, \quad \mathbf{b}_j = \mathcal{T}_{i,j}^{(-)}\mathbf{b}_{i-1} + \mathcal{R}_{i,j}^{(+)}\mathbf{a}_j. \tag{3.6}$$

Note that the phase changes have been encapsulated in these equations, and that the symmetries $\mathcal{R}_{i,j}^{(-)} = \mathcal{R}_{i,j}^{(+)}$ and $\mathcal{T}_{i,j}^{(-)} = \mathcal{T}_{i,j}^{(+)}$ cannot be assumed. Using these definitions, it is straightforward to show that the reflection and transmission matrices for rows i to $j+1$ can be obtained from those for rows i to j, and those for the individual row $j+1$ alone, through the identities

$$\mathcal{R}_{i,j+1}^{(-)} = \mathcal{R}_{i,j}^{(-)} + \mathcal{T}_{i,j}^{(+)}(\mathcal{I} - \mathcal{R}_{j+1}^{(-)}\mathcal{R}_{i,j}^{(+)})^{-1}\mathcal{R}_{j+1}^{(-)}\mathcal{T}_{i,j}^{(-)},$$

$$\mathcal{T}_{i,j+1}^{(+)} = \mathcal{T}_{i,j}^{(+)}(\mathcal{I} - \mathcal{R}_{j+1}^{(-)}\mathcal{R}_{i,j}^{(+)})^{-1}\mathcal{T}_{j+1}^{(+)},$$

$$\mathcal{R}_{i,j+1}^{(+)} = \mathcal{R}_{j+1}^{(+)} + \mathcal{T}_{j+1}^{(-)}(\mathcal{I} - \mathcal{R}_{i,j}^{(+)}\mathcal{R}_{j+1}^{(-)})^{-1}\mathcal{R}_{i,j}^{(+)}\mathcal{T}_{j+1}^{(+)},$$

and

$$\mathcal{T}_{i,j+1}^{(-)} = \mathcal{T}_{j+1}^{(-)}(\mathcal{I} - \mathcal{R}_{i,j}^{(+)}\mathcal{R}_{j+1}^{(-)})^{-1}\mathcal{T}_{i,j}^{(-)},$$

where $\mathcal{I}$ is the identity matrix of dimension $2N+1$. The reflection and transmission matrices for the entire array, $\mathcal{R}_{1,M}^{(\pm)}$ and $\mathcal{T}_{1,M}^{(\pm)}$, can thus be obtained by starting at row 1, for which

$$\mathcal{R}_{1,1}^{(-)} = \mathcal{E}_{1-}\mathcal{R}_1\mathcal{E}_{1-} \quad \text{and so on,}$$

and repeatedly applying the above identities. Discrete approximations of the reflected and transmitted amplitude functions, a and b, can then be found using the respective components of (3.6) with $(i, j) = (1, M)$. Although the solution throughout the domain Ω can be derived using the same equations, the calculation of these far-field response functions will be sufficient for the numerical investigation of attenuation in the following section.

4. Numerical results. The results that will be presented in this section are intended to demonstrate the effects of allowing for different periodicities (i.e., in-row spacings) between rows on wave attenuation through the array of scatterers. It is convenient to first nondimensionalize with respect to the wavenumber k, and for the remainder of our study $k \equiv \pi$. The periodicity parameter, $p = 2/s$, is then determined only by the nondimensional in-row spacing between adjacent obstructions, s.

From the construction of the problem and solution method given in sections 2–3 it is clear that the role of the incident angle is crucial to the structure of the wave field traveling through the array. For this reason the results that will be presented are of the modulus of the transmitted amplitude, $\mathcal{T} \equiv |b|$, as a function of the nondimensional angle parameter $u \in [-1, 1]$. Furthermore, the incident amplitude is set as $\iota(u) \equiv 1$. Although it has no physical relevance, this choice serves the current investigation well, as it does not influence the shape of the transmitted wave field.

The method outlined in section 3 is intended for an ensemble average of arrays composed of a large number of rows. This is so that unwanted resonant behaviors can be moderated. Nonetheless, it is informative to begin by studying how the method performs on simple one- and two-row arrays. One significant benefit of this is that, in certain cases, the wave interactions between rows can be calculated exactly.

The top panels of Figure 4.1 show the transmitted wave fields for rows with periodicity parameters $p = 4/3$ and $p = 5/3$, respectively. The bottom panels show the results for two-row arrays, composed of these rows in the given order, and with row spacings $q = 2$ and 4, respectively. Note that both rows generate multiple scattering angles for certain intervals of u. The radii of the scatterers in the rows is set as $r = 0.3s$. It is clear that for any combination of these rows the wave interactions will be calculated exactly if the discretization parameter, N, is chosen to be a multiple of 3. But the interest here is rather to observe the behavior of the approximation when N is chosen to be other values.

Convergence of the approximation is shown using the three values $N = 20$, 40, and 80. Exact values, calculated using $N = 24$, are also plotted. In the results for the individual rows it is evident that the exact transmitted amplitude is attained for a relatively small value of N, even in the intervals of multiple scattering angles.

For the two-row arrays, the situation is more complicated. Although the approximations capture the exact solution at most points, they struggle for certain isolated values. Unsurprisingly, these values correspond to the resonant points at which the number of scattering angles changes, and the poor performance here is to be expected, as the transmitted amplitude is highly sensitive around these points. It is the elimination of this type of sensitivity that is intended in the large arrays by allowing for different in-row spacings.

The investigation now turns to the intended application for the method—that of an ensemble average of arrays composed of a large number of rows. From here on, the number of rows is set as $M = 100$, as this is large enough to ensure that the appropriate attenuation properties are produced.

It is necessary at this juncture to identify three different regimes. The first is $p > 2$, for which multiple scattering angles are not generated by the array for any incident angle. In the second, $1 < p \leq 2$, and additional wave angles are produced for only certain intervals of wave angles. The final case is $p \leq 1$, so that multiple angles exist for every incident wave angle, although the number will change as this quantity is varied. Results are thus based on the three different mean periodicities, $p = 2.5$, 1.75, and 1, which represent the above regimes. It is simple to show that these values are given by the in-row spacings $s = 0.8$, $8/7$, and 2, respectively.

Previous investigations of wave attenuation through multiple-row arrays have been made with fixed periodicities [3, 15, 1]. It was demonstrated that, away from the resonant frequencies, by forming an ensemble average of a number of simulations that use identical geometries, but with row spacings selected from a normal distribution

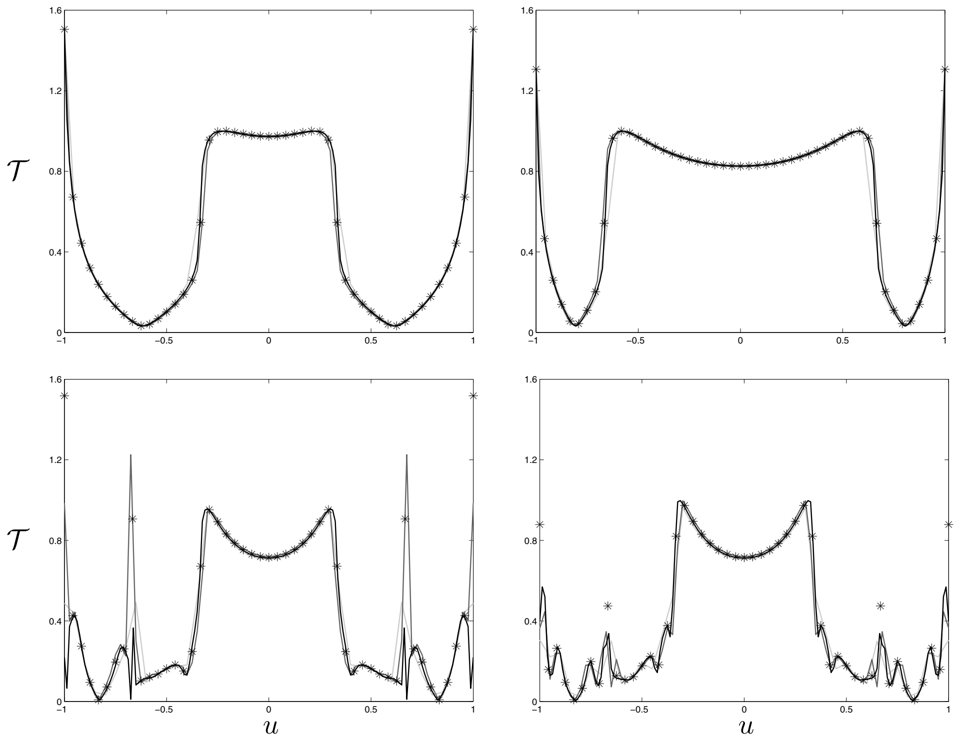

FIG. 4.1. *The transmitted wave field after $M = 1$ row (top panels) and $M = 2$ rows (bottom panels). The row used for the top left panel has periodicity parameter $p = 4/3$, and the row used for the top right panel has $p = 5/3$. The two-row arrays are composed of these rows, with row spacing $q = 2$ (bottom left) and $q = 4$ (bottom right). Three discretizations are shown for each panel, with $N = 20$ (light gray curves), $N = 40$ (dark gray), and $N = 80$ (black). Exact values are shown with symbols.*

with a sufficiently large standard deviation (the value of the mean is irrelevant), an exponential decay of wave energy is produced. This strategy avoids Bragg resonance, in which wave coherence due to a repeated row spacing creates transmission that is approximately full or absent after a small number of rows.

Benefitting from this understanding, the results presented in this section are derived from an ensemble average of 50 simulations, in which the distances between the rows are selected from a normal distribution (with standard deviation approximately $q/3$). New to this study is the ability to choose different in-row spacings, and here the values of the spacings and radii are taken from normal distributions, with mean values μ and ν, respectively. For the purpose of the current investigation the ratio $\nu/\mu = 0.25$ is set, so that it is necessary only to refer to the value of μ from here on. Results, which are not presented, confirm that this value does not affect the behaviors that will be observed. The corresponding standard deviations are given by $\sigma\mu$ and $\sigma\nu$, where the quantity σ is a chosen positive constant. The effects of changing the values of μ and σ is the principal component of this numerical investigation.

An efficient way of generating the ensemble average is to calculate and store the results for J single rows, where the geometries are selected from the desired normal distribution (μ, σ). Random permutations of these are then used to form the multiple-row arrays that comprise the ensemble average.

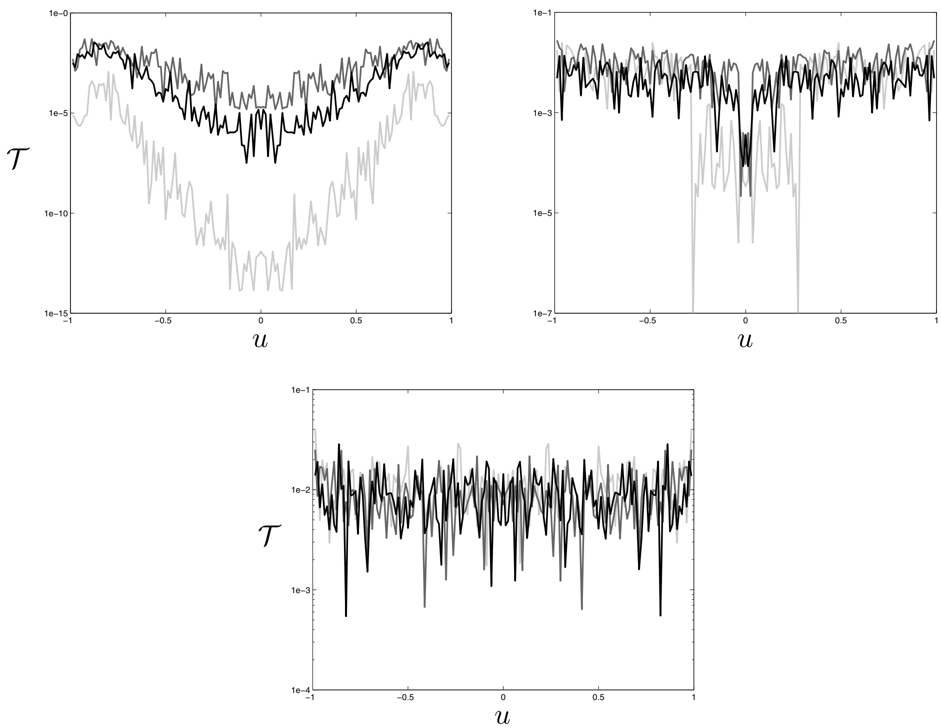

FIG. 4.2. *The transmitted wave field after $M = 100$ rows for different values of the number of single-row solutions, J, used in the ensemble average. The top left panel shows the case in which the mean in-row spacing is $\mu = 0.8$; the top right shows $\mu = 8/7$ and the bottom shows $\mu = 2$. The three values $J = 10$ (light gray curves), 30 (dark gray), and 50 (black) are shown for each. In all cases the standard deviation parameter is $\sigma = 0.4$ and the discretization is such that $N = 80$.*

In Figure 4.2 the value of J that is necessary to produce accurate representations of the transmitted wave fields is investigated. The different panels show the three cases indicated previously, with mean in-row spacings $\mu = 0.8$, $8/7$, and 2. Here, the standard deviation parameter is set as $\sigma = 0.4$, and the discretization of the angle parameter, which is investigated in Figure 4.3, is $N = 80$.

Results are shown for the three different values $J = 10$, 30, and 50. From these results, and others which are not presented, it appears that $J = 50$ is sufficient to give accurate results for the parameter regimes that will be used in this work, and this value is used for the remainder of our investigation. It is, however, interesting to note that the results are more sensitive for larger periodicities.

Before proceeding, it is important to verify that the numerical results obtained by implementing the method outlined in the previous section will converge as the discretization of the angle parameter is refined. To this end, in Figure 4.3 the convergence of the transmitted wave field with respect to the discretization parameter N is examined. As in the previous figure, the panels refer to the three different regimes, using mean in-row spacings $\mu = 0.8$, $8/7$, and 2, respectively, and the standard deviation parameter is set as $\sigma = 0.4$.

In each case, the four different discretizations $N = 10$, 20, 40, and 80 are shown. It is reasonable to deduce from these results that convergence of the transmitted wave

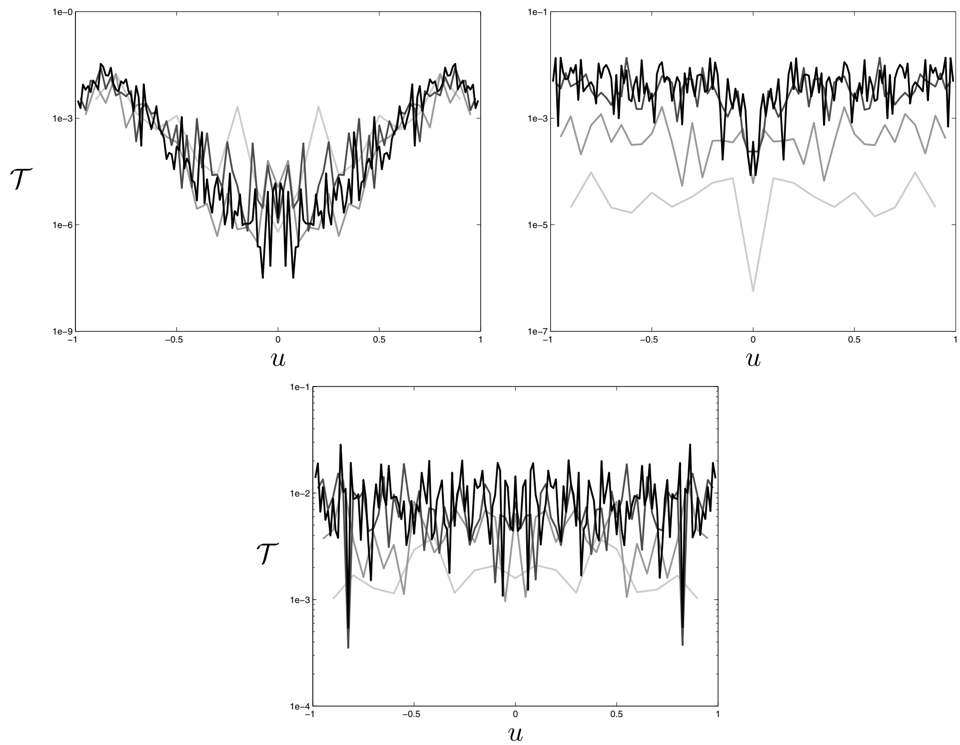

FIG. 4.3. *The convergence of the transmitted wave field after $M = 100$ rows with respect to the discretization parameter, N. The top left panel shows the case in which the mean in-row spacing is $\mu = 0.8$; the top right shows $\mu = 8/7$, and the bottom shows $\mu = 2$. The four values $N = 10$ (light gray curves), 20 (mid gray), 40 (dark gray), and 80 (black) are shown for each. In all cases the standard deviation parameter is $\sigma = 0.4$ and the number of single-row solutions used is $J = 50$.*

fields is achieved as N is increased and that $N = 80$ is sufficient to produced accurate data. This value is therefore maintained in the numerical results that follow.

It is interesting to note that the second case, $\mu = 8/7$, is most responsive to the refinement of the discrete system. This can be attributed to the sensitivity of the transmitted wave field to the angle parameter when the first additional wave angle cuts in, which will be highlighted in Figure 4.5. Another feature of the convergence shown in Figure 4.3 is the tendency for coarse discretizations to overestimate the attenuation produced when multiple waves are present. This is likely to be caused by an insufficient representation of the reflection and transmission produced by the individual rows around the resonant points.

Having established some confidence in the solution method and numerical routine, we now move to the primary objective, which is investigating the effects of allowing for differing periodicities between the rows on wave attenuation. Thus, Figures 4.4–4.6 show how the transmitted wave fields are modified by an increasing level of variation in the in-row spacings for the mean values $\mu = 0.8$, $8/7$, and 2, respectively. In each figure the top left panel shows the case in which the periodicity is fixed ($\sigma = 0$), and the cases $\sigma = 0.1$, 0.2, and 0.4 are shown by the top right, bottom left, and bottom right panels, respectively.

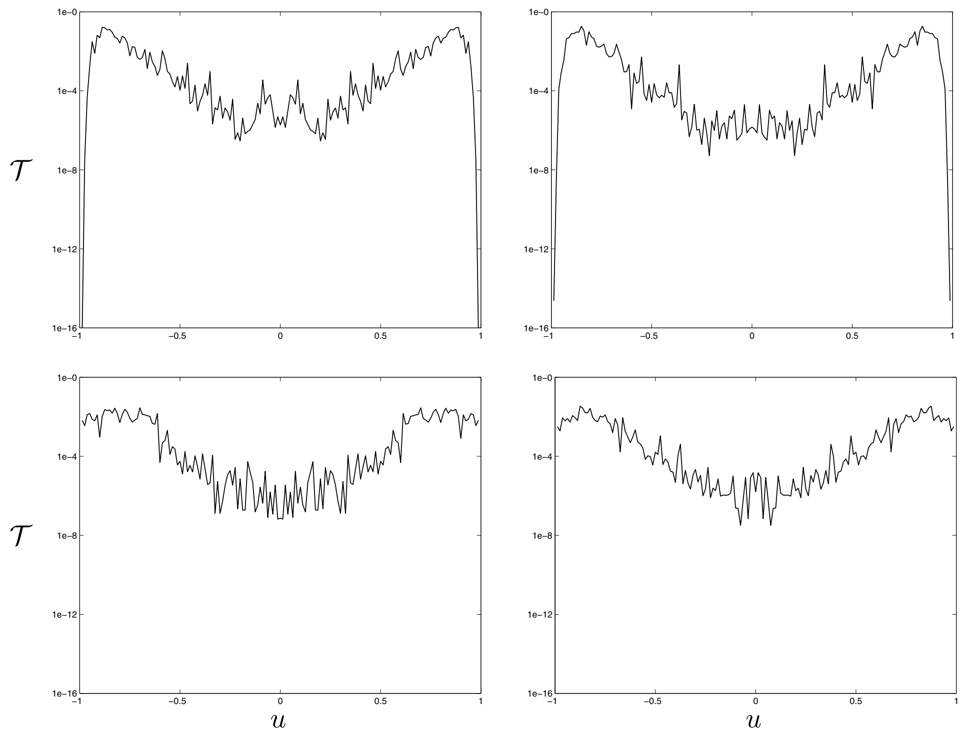

FIG. 4.4. *The effects of allowing variation in the periodicity of the rows on the transmitted wave field, with mean in-row spacings $\mu = 0.8$. The top left panel shows the case in which no variation is included ($\sigma = 0$); the top right shows $\sigma = 0.1$, the bottom left $\sigma = 0.2$, and the bottom right $\sigma = 0.4$. In all cases the discretization is such that $N = 80$ and the number of single-row solutions is $J = 50$.*

For the situation displayed in Figure 4.4, the mean periodicity produces no additional scattered wave angles for all incident angles. It is therefore unsurprising to see that adding some variation to the spacing has little effect on the magnitude and shape of the transmitted wave field. This retains its concave appearance, with attenuation decreasing as the incident wave angle moves away from normal incidence ($u = 0$). Increasing the level of variation, so that some rows that produce multiple scattering angles are present, does have the one notable effect of smoothing away the sharp drop to zero in the transmitted wave energy as grazing incidence is approached ($u = \pm 1$).

In Figure 4.5 the mean periodicity generates an additional scattered wave angle only on the intervals $|u| \geq 0.75$. It is clear from the transmitted wave field shown in the top left panel, in which the in-row spacings of the rows in the array are identical, why problems in calculating attenuation have been encountered around the resonant points in previous studies. Within the interval in which no multiple wave angles occur, $|u| < 0.75$, the transmitted wave field resembles those of the previous figure. However, when additional waves cut in, there is a sharp drop in the transmission of between 30–40 orders of magnitude over an interval of approximately 0.05 in u, and it is followed by volatile, spiky behavior as the incident wave angle is increased. In these double wave angle intervals it would be very hard to ascertain a meaningful attenuation rate, as the wave field is extremely sensitive to the incident wave angle.

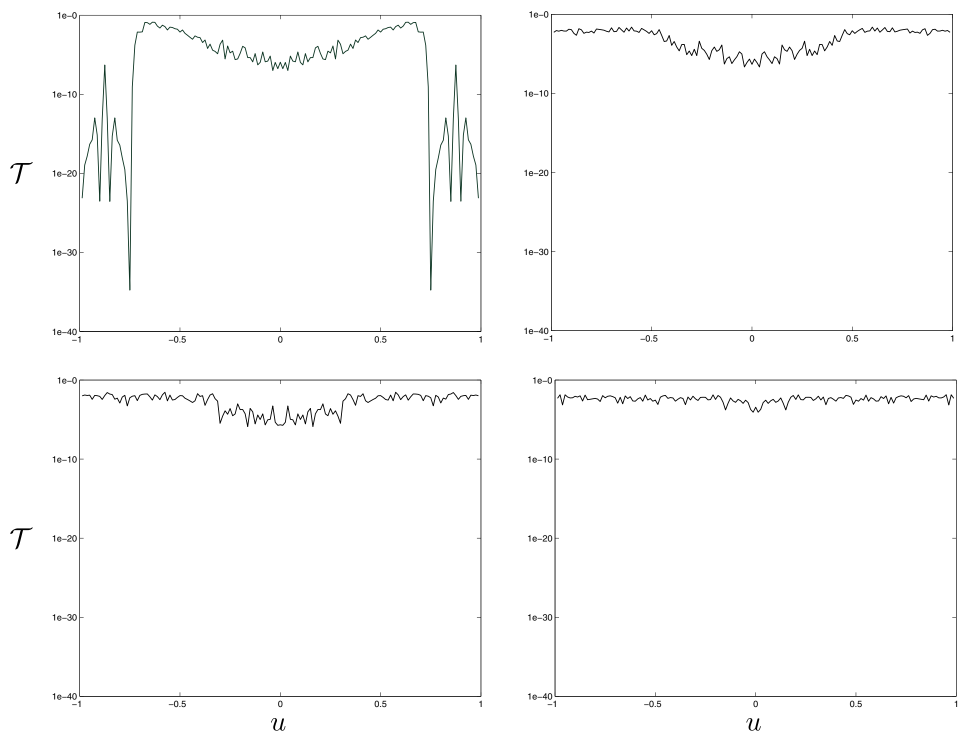

FIG. 4.5. *As in Figure* 4.4 *but with mean in-row spacings* $\mu = 8/7$.

Despite this highly unsettled behavior for a fixed periodicity, a dramatic smoothing is created by the introduction of only a small proportion of variations in the in-row spacings. With $\sigma = 0.1$, as the resonant angles are approached from below, the transmitted amplitude levels out to a relatively constant value. Conversely, for the majority of the interval in which only a single scattering angle exists, the wave field is not significantly altered by using $\sigma = 0.1$. However, as the variation is increased, the concavity of the wave field here is also smoothed away. The result is that with $\sigma = 0.4$, the transmitted wave field is almost completely insensitive to direction, and its average magnitude is in the range of $\mathcal{T}$, which was calculated in the single scattering angle interval for the fixed periodicity case.

Figure 4.6 shows results for the regime in which the mean periodicity produces multiple wave angles for all incident angles. Unsurprisingly, for the fixed periodicity case the transmitted wave field is again highly unsettled, although in this case the ordinate axes range only over 20 orders of magnitude. It may therefore be speculated that the sensitivity of the transmitted wave field is greatest when the first additional wave angle cuts in.

Here it is striking that only a small proportion of variations in the in-row spacings of the rows is required to produce a settled transmitted wave field. Increasing the variation further appears to be inconsequential. As with the previous case ($\mu = 8/7$), the transmitted wave field produced when variation in the in-row spacings is permitted is insensitive to direction. Its average magnitude is comparable to the higher end of the range of the values of $\mathcal{T}$ attained when the periodicity is fixed.

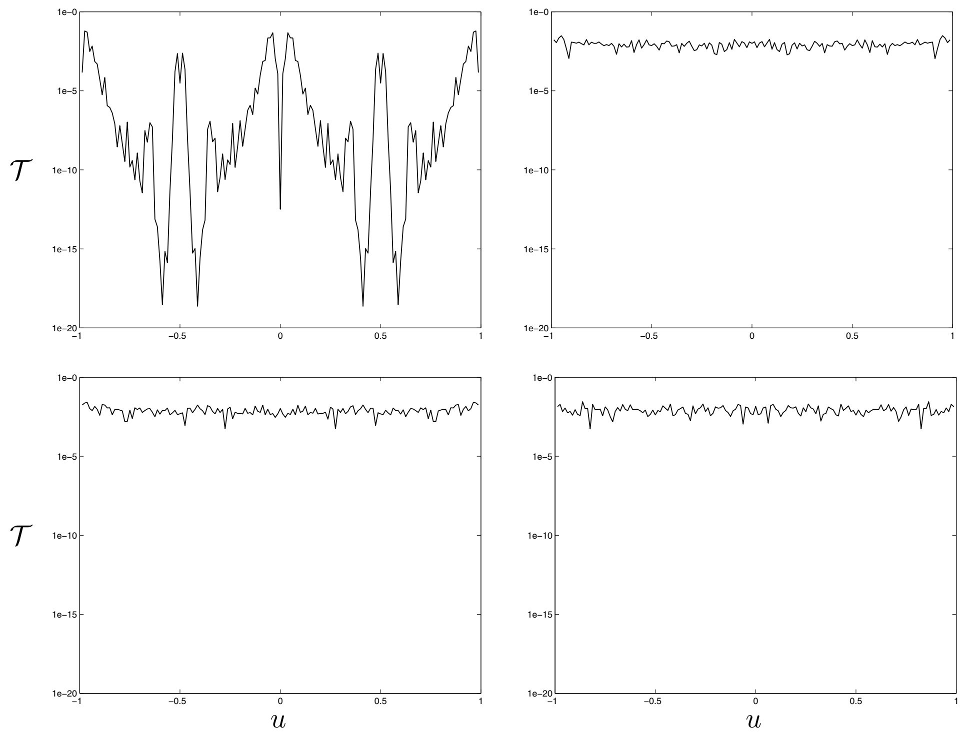

FIG. 4.6. *As in Figure* 4.4 *but with mean in-row spacings* $\mu = 2$.

5. Summary and conclusions. The investigation conducted in this work was motivated by the difficulties encountered in previous studies when attempting to calculate the attenuation rate of waves traveling through arrays composed of multiple rows of scatterers. In this setting, each row contains an infinite number of equispaced, identical obstructions, so that periodicity may be invoked to calculate its scattering response to an incident plane wave at a given angle.

An existing solution method was adapted to allow for the freedom of having an array composed of rows with different periodicities. The method was applied to a canonical problem, in which a potential function exists in a two-dimensional plane exterior to the array, and satisfies a Neumann condition on the circumferences of the circular scatterers. Forcing is provided by an incident wave that propagates from the far-field towards the array.

For an individual row, the scattered wave field can be expressed as the sum of a finite number of propagating waves and an infinite number of evanescent waves. The set of scattering angles, at which the propagating waves travel, is determined by a relationship between the forcing wave and the periodicity of the row. If a consistent periodicity is maintained in all rows of the array, then interactions between the rows are confined to the set of scattering angles generated by the individual rows, and hence the single-row solutions can be composed in a straightforward manner to determine the overall scattering of the array. However, if different periodicities are permitted, then the interactions generate waves that travel at angles not present in the scattered fields of the individual rows, unless they are multiples of one another. For an array composed of a large number of randomized rows it is tedious and inefficient to track the set of scattering angles, and it may become infinite. Instead, a method was proposed, which is based on a discretization of the directional spectrum followed by a projection of the geometry of each row onto the corresponding mesh. This essentially assigns an artificial periodicity to the entire array that gets larger as the mesh is refined and the geometry approaches its natural state. Given a discretization, the set of scattering angles for any number of rows is generated by this known periodicity, and the response of the entire array can be calculated from the solutions of its constituent rows in an iterative manner. A wide spacing approximation was also applied to simplify the interactions between adjacent rows.

Numerical calculations of the transmitted wave fields produced by the method were then given. To begin with, a set of simple one- and two-row arrays was used. This allowed the discretization to be chosen so that the wave interactions would be exact. These exact results were compared with approximations formed by different discretizations. It was seen that the approximations gave high accuracy, even for coarse discretizations, except close to the resonant points.

The remainder of the numerical results were calculated from ensemble averages in which the row spacings and in-row spacings were chosen from normal distributions with a given mean and standard deviation. Convergence of the results was established for both the number of single-row solutions required in the ensemble average and the discretization of the directional spectrum. Three situations were considered, in which the mean periodicities correspond to arrays that produce multiple scattered wave angles for (i) no incident wave angles; (ii) only certain intervals of incident wave angles; and (iii) all incident wave angles. It was evident from the results for arrays in which the in-row spacings were fixed why difficulties were encountered in previous studies when seeking an attenuation rate. Allowing for in-row spacing variation in situation (i) did little but to smooth the sharp drop in the transmitted amplitude as grazing incidence is approached. However, for situations (ii)–(iii) the addition of variation in the in-row spacing had a fundamental effect on the transmitted wave field, smoothing the erratic behavior produced by the multiple scattered wave angles, and resulting in a wave field that appeared insensitive to direction.

The ramifications of this work for studies of wave attenuation through multiple-row arrays is clear. The findings will be most significant for applications in which the structure of the scatterers is in some sense randomized, such as ice floes in the marginal ice zone, which was the stimulus for this work. Before considering such an undertaking, it would be prudent to investigate the effects of easing the wide spacing approximation to allow for some influence of the least rapidly decaying waves on the interactions between rows.

Appendix. Solutions for individual rows at single and double resonance. Here modifications are considered that must be made at resonant points to the integral equation solution method for an individual, outlined in section 3.1. As in section 3.1, let the radius of the obstructions be denoted r and the in-row spacing be s. Forcing is provided by a plane incident wave, with wavenumber k, which propagates from $x \to -\infty$ at the oblique angle τ. The method that is employed at the resonant points is adapted from that of [10], which dealt with modifications to a solution method for an individual row based on Graf's addition formula.

Resonance indicates that there exists either one or two zeros in the set

$$\{v_j : v_j = \sqrt{1-u_j^2}, j \in \mathbb{Z}\}, \quad u_j = u_0 + pj,$$

where $u_0 = \sin\tau$ and $p = 2\pi/ks$. The definition of the quasi-periodic Green's function G given in (3.2) clearly displays that it is singular at these points. However, the potential ϕ, defined in integral form by (3.3), which is a physical quantity, can be expected to remain bounded, and the modifications to the solution method are based on this premise.

A.1. Single resonance. Suppose that there exists an index m for which $v_m = 0$, so that $|u_m| = 1$, and all other $v_j \neq 0$. Define a modified Green's function $\widetilde{G}_{\mathcal{M}}$ as

$$\widetilde{G}_{\mathcal{M}}(\mathbf{x}|\mathbf{X}) = \frac{1}{2\mathrm{i}ks} \sum_{j\in\mathbb{Z}/\mathcal{M}} \frac{1}{v_j} \mathrm{e}^{\mathrm{i}kv_j|x-X|-\mathrm{i}ku_j(y-Y)},$$

and the function $g(\mathbf{x} : u) = \mathrm{e}^{\mathrm{i}kuy}$, so that at the resonant point we may write

$$G(\mathbf{x}|\mathbf{X}) = \widetilde{G}_m(\mathbf{x}|\mathbf{X}) + \frac{1}{2\mathrm{i}ksv_m} g(\mathbf{X} : u_m) g(\mathbf{x} : -u_m),$$

which isolates the singular term in G. In order for the integral appearing on the right-hand side of (3.3) to be bounded, the expansion

$$I_m(v_m) = c_1 v_m + c_2 v_m^2 + \cdots, \tag{A.1}$$

where

$$I_j = \int_{-\pi}^{\pi} \left[\big(\partial_n g(\mathbf{x} : -u_j)\big) \phi(\mathbf{x}) \right]_{|\mathbf{x}|=r} \,\mathrm{d}\theta,$$

is required to hold in a vicinity of the resonant point. We are therefore left with two integral expressions,

$$\epsilon\phi(\mathbf{X}) = \phi_i(\mathbf{X}) - r \int_{-\pi}^{\pi} \left[\big(\partial_n \widetilde{G}_m(\mathbf{x}|\mathbf{X})\big) \phi(\mathbf{x}) \right]_{|\mathbf{x}|=r} \,\mathrm{d}\theta - \frac{r}{2\mathrm{i}ks} c_1 g(\mathbf{X} : u_m) \quad (\mathbf{X} \in \Omega_0)$$

and

$$I_m(0) = 0,$$

to calculate the function ϕ and constant c_1. When solving these equations via a Fourier expansion of the azimuthal coordinate, it is useful to note that

$$\frac{1}{2\pi} \int_{-\pi}^{\pi} g(\mathbf{x} : \pm 1) \mathrm{e}^{-\mathrm{i}\alpha\theta} \,\mathrm{d}\theta = \mathrm{J}_\alpha(\pm kr), \quad \frac{1}{2\pi} \int_{-\pi}^{\pi} \big(\partial_n g(\mathbf{x} : \pm 1)\big) \mathrm{e}^{-\mathrm{i}\alpha\theta} \,\mathrm{d}\theta = \partial_n \mathrm{J}_\alpha(\pm kr)$$

for $|\mathbf{x}| = r$, where J_α is the Bessel function of the first kind, order α.

A.2. Double resonance. In this case there exist two indices m and n for which $v_m = 0$ and $v_n = 0$ simultaneously. Without loss of generality, it can be assumed that $u_m = -1$ and $u_n = 1$. The construction of the solution method under such circumstances is similar to that of the single resonance case, but now the following expansion must be imposed:

$$I_n(v_n) = d_1 v_n + d_2 v_n^2 + \cdots,$$

in addition to (A.1). The three integral expressions,

$$\epsilon\phi(\mathbf{X}) = \phi_i(\mathbf{X}) - r\int_{-\pi}^{\pi} [\big(\partial_n \widetilde{G}_{m,n}(\mathbf{x}|\mathbf{X})\big)\phi(\mathbf{x})]_{|\mathbf{x}|=r}\, \mathrm{d}\theta - \frac{r}{2\mathrm{i}ks}\big(c_1 g(\mathbf{X}:-1) + d_1 g(\mathbf{X}:1)\big)$$

for $\mathbf{X} \in \Omega_0$,

$$I_m(0) = 0, \quad \text{and} \quad I_n(0) = 0,$$

can then be solved to obtain the function ϕ and constants c_1 and d_1.

Acknowledgment. I wish to thank Timothy Williams for his advice on the presentation of this work.

REFERENCES

[1] L. G. Bennetts, M. A. Peter, V. A. Squire, and M. H. Meylan, *A three-dimensional model of wave attenuation in the marginal ice zone*, J. Geophys. Res., 115 (2010), C12043.

[2] L. G. Bennetts and V. A. Squire, *Linear wave forcing of an array of axisymmetric ice floes*, IMA J. Appl. Math., 75 (2009), pp. 108–138.

[3] L. G. Bennetts and V. A. Squire, *Wave scattering by multiple rows of circular ice floes*, J. Fluid Mech., 639 (2009), pp. 213–238.

[4] T. Chou, *Band structure of surface flexural-gravity waves along periodic interfaces*, J. Fluid Mech., 369 (1998), pp. 333–350.

[5] R. A. Dalrymple, S. N. Seo, and P. A. Martin, *Water wave scattering by rows of circular cylinders*, in Proceedings of the 21st International Coastal Engineering Conference, Coata del Sol-Malaga, Spain, B. L. Edge, ed., 1988, pp. 2216–2228.

[6] M. A. Heckl and L. S. Mulholland, *Some recent developments in the theory of acoustic transmission in tube bundles*, J. Sound Vibration, 179 (1995), pp. 37–62.

[7] C. M. Linton, *The Green's function for the two-dimensional Helmholtz equation in periodic domains*, J. Engrg. Math., 33 (1998), pp. 377–402.

[8] C. M. Linton and D. V. Evans, *The interaction of waves with a row of circular cylinders*, J. Fluid Mech., 251 (1993), pp. 687–708.

[9] C. M. Linton, R. Porter, and I. Thompson, *Scattering by a semi-infinite periodic array and the excitation of surface waves*, SIAM J. Appl. Math., 67 (2007), pp. 1233–1258.

[10] C. M. Linton and I. Thompson, *Resonant effects in scattering by periodic arrays*, Wave Motion, 44 (2007), pp. 165–175.

[11] P. McIver, *Water-wave propagation through an infinite array of cylindrical structures*, J. Fluid Mech., 424 (2000), pp. 101–125.

[12] R. C. McPhedran, L. C. Botten, A. A. Asatryan, N. A. Nicorovici, P. A. Robinson, and C. M. de Sterke, *Calculation of electromagnetic properties of regular and random arrays of metallic and dielectric cylinders*, Phys. Rev. E (3), 60 (1999), pp. 7614–7617.

[13] N. A. Nicorovici, R. C. McPhedran, and R. Petit, *Efficient calculation of the Green's function for electromagnetic scattering by gratings*, Phys. Rev. E (3), 49 (1994), pp. 4563–4577.

[14] M. A. Peter and M. H. Meylan, *Water-wave scattering by a semi-infinite periodic array of arbitrary bodies*, J. Fluid Mech., 575 (2007), pp. 473–494.

[15] M. A. Peter and M. H. Meylan, *Water-wave scattering by vast fields of bodies*, SIAM J. Appl. Math., 70 (2009), pp. 1567–1586.

[16] R. Porter and D. V. Evans, *Rayleigh-Bloch surface waves along periodic gratings and their connection with trapped modes in waveguides*, J. Fluid Mech., 386 (1999), pp. 233–258.

[17] R. Porter and D. Porter, *Interaction of water waves with three-dimensional periodic topography*, J. Fluid Mech., 434 (2001), pp. 301–335.

[18] Lord Rayleigh, *On the dynamical theory of gratings*, Proc. R. Soc. Lond. A, 79 (1907), pp. 399–416.

[19] V. A. Squire and S. C. Moore, *Direct measurement of the attenuation of ocean waves by pack ice*, Nature, 283 (1980), pp. 365–368.

[20] I. Thompson, C. M. Linton, and R. Porter, *A new approximation method for scattering by long finite arrays*, Quart. J. Mech. Appl. Math., 61 (2008), pp. 333–352.

[21] V. Twersky, *On scattering of waves by the infinite grating of circular cylinders*, IRE Trans. Antennas and Propagation, 10 (1962), pp. 737–765.